IOP Conf. Series: Materials Science and Engineering **400** (2018) 082016 doi:10.1088/1757-899X/400/8/082016

Numerical study on motions of a containership on head waves

S Pacuraru, L Domnisoru and F Pacuraru
Department of Naval Architecture
"Dunarea de Jos" University of Galati, Domneasca Street 111, 800201, Romania

E-mail: florin.pacuraru@ugal.ro

Abstract. Seakeeping performance represents an important chapter in the study of ship hydrodynamics. Computation of ship motions, amplitudes and accelerations conducts to the prediction of ship safety and security during operation. The experimental measurements of ship motions on regular waves are considered accurate methods, but still expensive. The paper presents the study of motions of a container ship in head regular and irregular waves. The 3D numerical analysis is performed based on BEM boundary element method, a CFD computational fluid dynamics method. In the numerical approach, seakeeping analysis was performed by using potential flow method. The comparison of numerical results for heave and pitch motions with the benchmark experimental tests reveals the accuracy and the validation of the numerical method. The numerical CFD–BEM investigation of ship motions at two forward speeds, 12 respectively 24 knots, were performed for the ship length to wave-length ratio in a range of 0.5–1.95. Based on the irregular wave results and by seakeeping limit criteria, the container ship navigation limits in head waves are analysed. The study results are pointing out good agreement between numerical and experimental models, the methodology being for practical design.

1. Introduction

Ship safety level is defined by statistic rules and verified by operational experience. Used successfully in past years, semi-empirical design cannot be used with confidence in establishing the hydrodynamic behaviour of the new shape design ships.

Approaching the hydrodynamic ship response in waves, seakeeping performance represents an important chapter. Computation of ship motions and wave induced loads conducts to the prediction of ship safety and security during operation.

The present work is focused on studying the ship motions in regular waves, comparing the ship response with experimental model data [1]. Also, a short-term ship statistical response in irregular waves considering an ITTC wave spectrum [2] is done. The results are analysed in terms of response amplitude operators for heave and pitch motions of ship in regular waves and the most probable amplitudes (RMS) in irregular waves. The waves are considered in head condition, resulting only the motions in the vertical ship's plane, heave and pitch.

The main dimension of the container ship used for the numerical model are presented in table 1 [1] and the ship hull details are presented in figures 1-3.

Content from this work may be used under the terms of the Creative Commons Attribution 3.0 licence. Any further distribution of this work must maintain attribution to the author(s) and the title of the work, journal citation and DOI.
Published under licence by IOP Publishing Ltd

Table 1. Main dimensions of the considered container ship [1].

Dimension	***Symbol***	***Value***
Length between perpendiculars	L_{pp}	230.0 m
Length of waterline	L_{WL}	232.5 m
Maximum beam of waterline	B_{WL}	32.2 m
Depth	D	19.0 m
Draft average	T	10.8 m
Displacement volume	∇	52030 m^3
Wetted hull surface	S_W	9422 m^2
Block coefficient	C_B	0.6505
Moment of Inertia around Ox axis	K_{xx}/B	0.40
Moment of Inertia around y, z axis	K_{yy}/L_{PP}, K_{zz}/L_{PP}	0.25
Longitudinal Centre of Buoyancy	LCB (%L_{PP})	-1.48
Service speed	U	24 knots

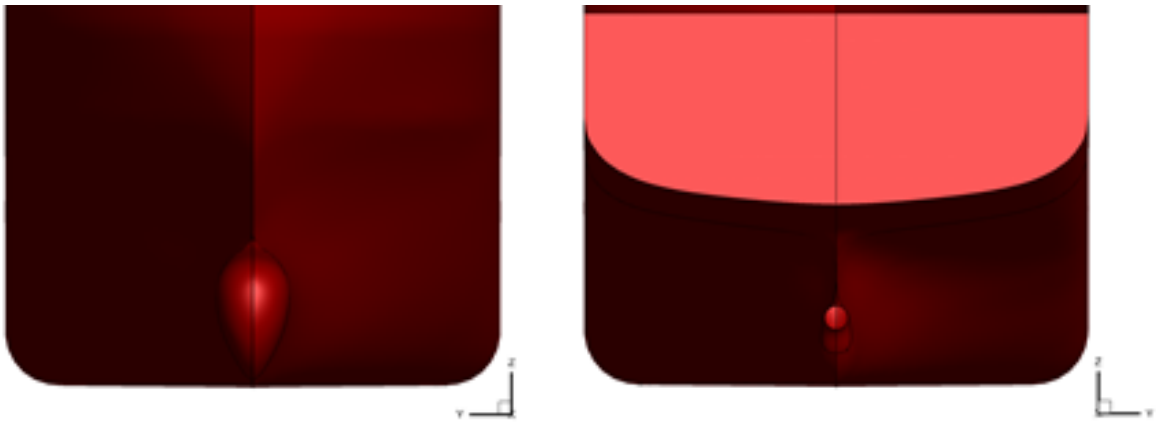

Figure 1. Container ship hull. Bow view (left) and stern view (right).

2. Computational methodology

The specific tools for seakeeping analysis evolved from Kriloff approaches to 2D strip theory slender body approached by Newman, Ogilvie, Salvesen, Tuck, Faltinsen [3,4]. A 3D-BEM boundary element method was initially attempted by Hess and Smith [5]. The actual 3D-BEM boundary element method [6] uses either Green's function or a Rankine source, as a source potential to satisfy boundary conditions [7]. The CFD methods based on 3D-BEM boundary element method have the advantage of considering even significant geometric hull nonlinearities, also making possible to have viscous and extreme flow simulation.

The computer program used is Shipflow Motions [8], a fully nonlinear potential flow solver for ship motions and added wave resistance, considering both regular and irregular waves conditions.

Having defined a correct geometry of the body, followed by an appropriate dimensioning of the computing domain, the next step in the numerical solution of the flow around the ship is the meshing of the hull surface. In the case of potential flow only the boundaries of the domain are going to be meshed. The numerical simulation technique of free surface fluid flow around the ship consists of a potential flow approach. The problem modelled by field equation (Laplace) and boundary conditions is solved by an integral method [8], in which the sources are distributed partly on the hull, and partly on the water free surface. The integration is not made on the entire domain, only on the boundary of the surface. That is the reason why it will be meshed only the hull and the free surface, which will reduce the pre-processing time, with lower accuracy than the methods including a full viscous flow approach.

The calculations are done for surface domain of one ship length upstream, two ship lengths downstream, the width of the free surface is one ship length, as depicted in figure 2. The hull is meshed using 47266 (43x140) BEM panels, presented in figure 3. The free surface has a mesh distribution of 380 panels per wave length (x direction) and 80 panels in y direction.

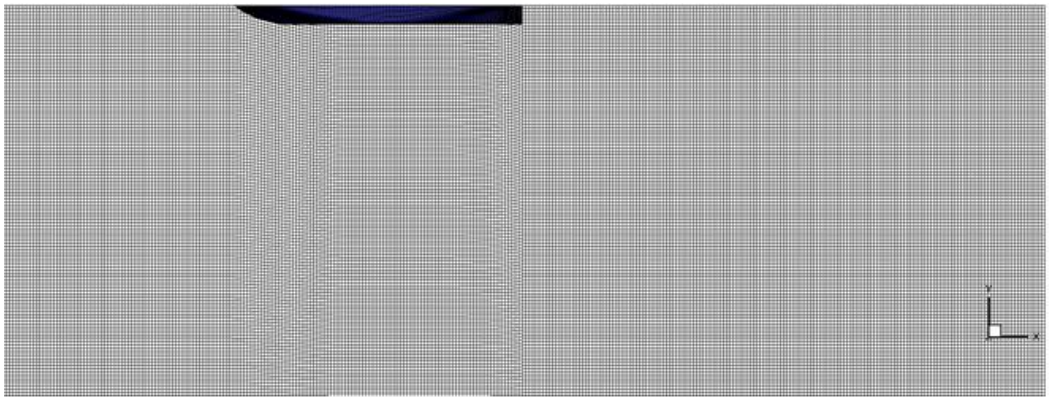

Figure 2. Water free-surface meshing.

Free surface initial model is a Bernoulli wave. For the ship motions in regular waves the program uses regular long-crested wave based on 5th-order Stokes' wave theory. The simulation will continue until convergence of equilibrium between ship and wave is obtained. Usually for analysis 10-15 wave encounter frequencies are required. The program computes several data, such as harmonic amplitudes and phases of the motions and resistance, as well as the response amplitude operators *RAO*. In case of irregular waves time records are computed and in ASCII files exported. The spectral response is obtained by a FFT approach using an in-house code [9].

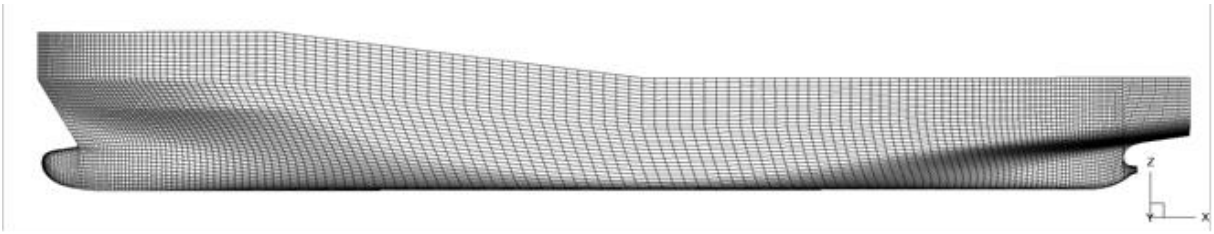

Figure 3. Hull surface meshing by BEM method.

3. Hydrodynamic ship response in regular waves

The computations for seakeeping in regular waves were performed for two cases of ship speed, respectively 12 and 24 knots. The considered incident waves are the 5th order Stokes waves with the heading angle β=180 deg., meaning that the wave propagates in opposite of the ship navigation direction. The L_{pp}/λ ratio is selected in range of 0.5 to 1.95. The regular wave height H_w is in rage of 1.9 to 7.5 m and the circular wave frequency is between 0.37 and 0.73 rad/s. The CFD program calculates the diffraction forces and moments generated by the regular waves and response amplitude operators *RAO* of ship's motions.

The analyzed results in the present study concern the heave (the translation along *X* axis) and the pitch (the rotation around *Y* axis) motions. The motions are calculated considering the ship advancing in regular waves on constant forward speed.

The response amplitude operators *RAO* for are defined as the ratio between the first motion harmonic and the regular wave amplitude.

Figure 4 presents the CFD results obtained in the case of head waves (β=180 deg.) for the ship speed of 12 knots and regular waves condition.

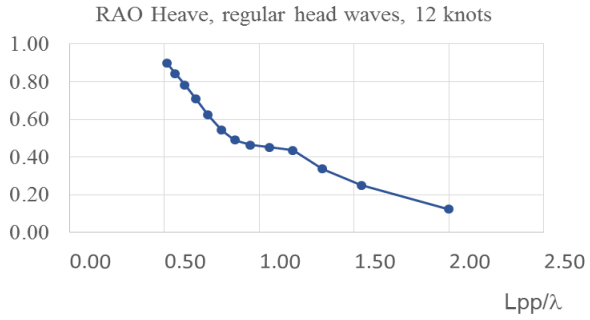

Figure 4a. RAO [m/m] heave motion in regular waves, $\beta = 180$ deg., speed 12 knots.

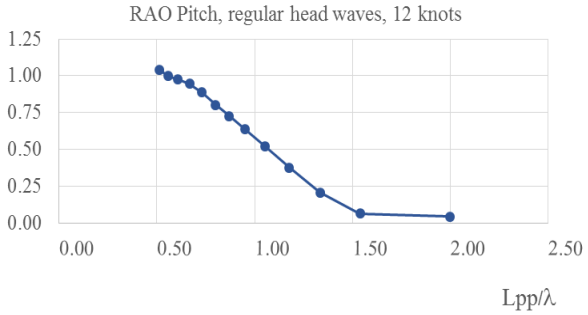

Figure 4b. RAO [deg/m] pitch motion in regular waves, $\beta = 180$ deg., speed 12 knots.

It can be observed that for a speed of 12 knots the ship has a maximum response when the wave length is double than the ship length, which corresponds to a low wave frequency. The ship response decreases with wave length and after $L_{pp}/\lambda \geq 2$, the value of *RAO*s became very small, so that over that value the dynamic response can be neglected. In figure 5 is given the comparison of experimental results (EFD) with the computational ones (CFD), for the regular head waves, for speed 24 knots.

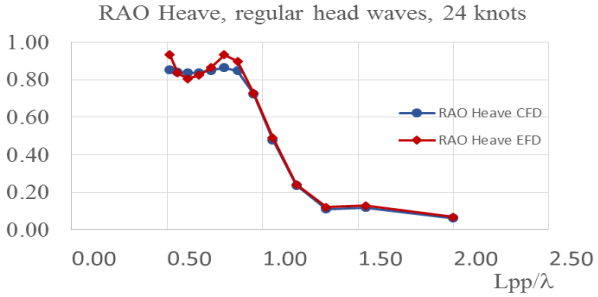

Figure 5a. RAO [m/m] heave for ship speed 24 knots, head regular waves. EFD-CFD comparison.

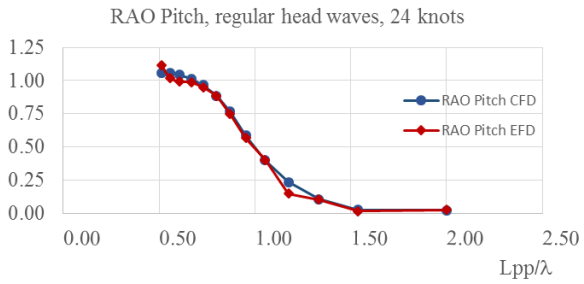

Figure 5b. RAO [deg/m] pitch for ship speed 24 knots, head regular waves. EFD-CFD comparison.

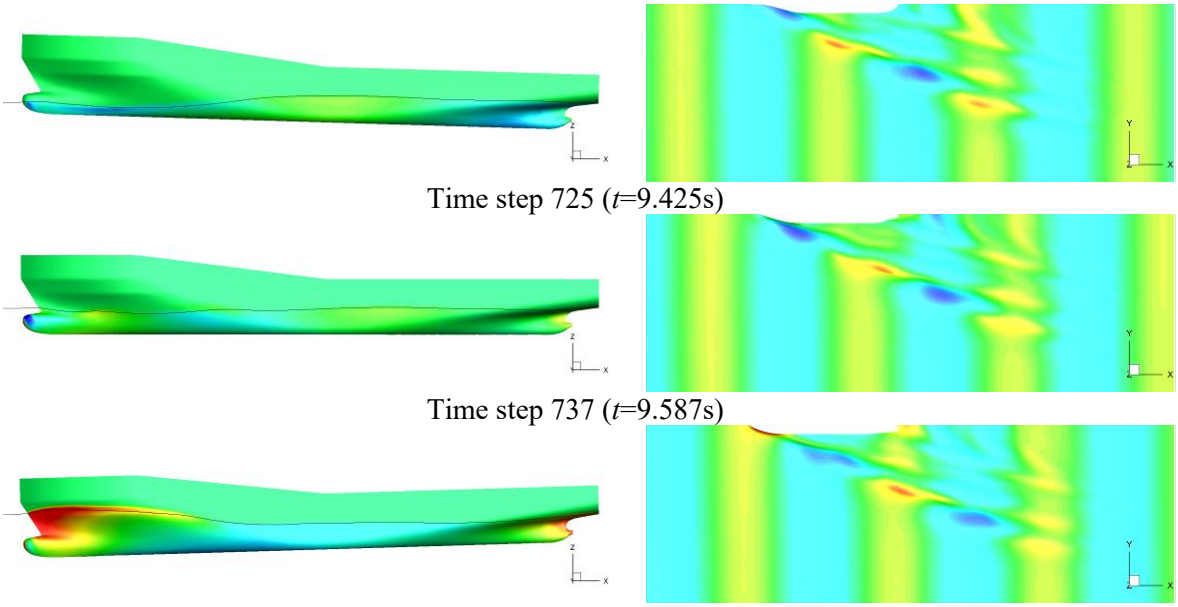

Time step 725 (t=9.425s)

Time step 737 (t=9.587s)

Time step 750 (t=9.75s)

Figure 6. Pressure distribution over the ship hull, regular head waves Lpp/λ=0.95.

The diagrams from figures 4,5.a,b show that the maximum values of heave and pitch *RAOs* are present for sub- unitary values of L_{pp}/λ ratio. The peak value of heave motion is at L_{pp}/λ=0.8, which corresponds to a wave circular frequency of 0.46 rad/s, while the peak value for pitch motion is at L_{pp}/λ=0.56, which corresponds to a wave circular frequency of 0.38 rad/sec. For the higher frequency domain or $L_{pp}/\lambda \geq 1$ it can be observed that the values for both motions are significant decreased, so that the dynamic response can be neglected. Comparing the CFD results with experimental data EFD one may observe that the differences appear in the lower frequency domain $L_{pp}/\lambda \leq 1$, while in higher frequency domain, the differences become smaller. In fact, for heave motion the curves are very similar. In figure 6 the pressure distribution over the hull is depicted, for the case of L_{pp}/λ=0.95.

4. Hydrodynamic ship response in irregular waves

This study continues with the short term prediction of ship hydrodynamic response in irregular waves by direct time domain computation of heave and pitch motion for the ship advancing in irregular head waves. The wave power density spectrum is the standard *ITTC* wave [2], presented in figure 7. In figure 8 is given the container ship in irregular wave, sea state *S7*.

The wave state is denoted by *S2*….*S7* (see Table 2, first three rows) describing the sea state from a moderate state *S2* to a developed sea state *S7*. The significant wave height is denoted by H_s having values from 0.3 to 7.5 m, and the zero-crossing wave period, T_z = 5.3….10.7s.

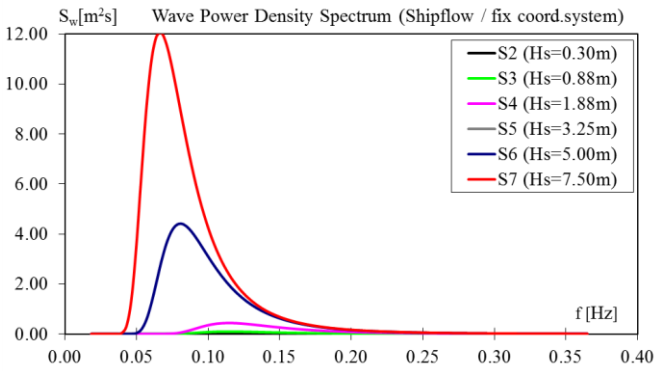

Figure 7. ITTC wave spectrum [2].

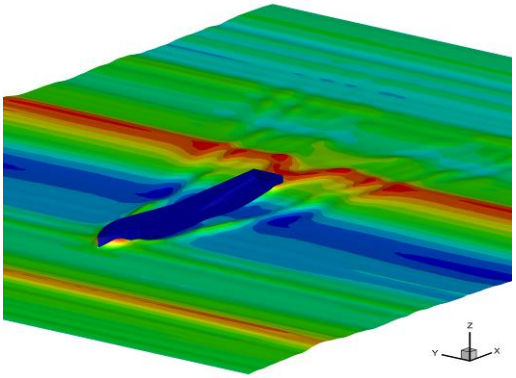

Figure 8. Container ship in irregular waves, reference sea state *S7*.

The heave in terms of power density spectrum is presented in figures 9a,b, for two different sea states, respectively *S4* (*Hs*=1.88 m) and *S7* (*Hs*=7.5 m). In figures 9,c,d are given the heave amplitudes for the same wave conditions. Due to the complex irregular wave expression combined also with the hull geometric nonlinearities, the spectral results include a wide number of components.

Analogues, in figures 10a,b is given the pitch motion, presented in terms of power density spectrum, for two different sea state, respectively *S4* (*Hs*=1.88 m) and *S7* (*Hs*=7.5 m) and in figures 10c,d are given the pitch amplitudes for the same wave conditions. The dynamic response includes a wide range of spectral components.

In the same way are presented below, in figures 11 and 12 the heave and pitch power density spectrum and amplitudes respectively for the maximum speed case of 24 knots, and the *S4* and *S7* irregular wave sea states.

The seakeeping analysis must include an analysis dedicated to limit criteria given by the classification societies. The statistical values obtained for the heave and pitch motions of the vessel have to be compared with the admissible limits for this specific container ship. The seakeeping criteria are formulated in terms of root mean square RMS_{max} most probable short-term statistical values for heave (RMS_{heave}) and pitch (RMS_{pitch}) motions.

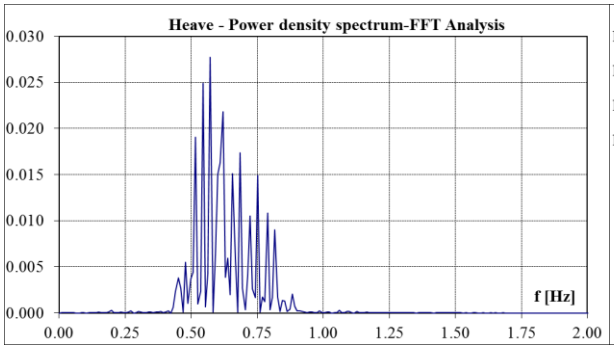

Figure 9a. Power density spectrum, heave motion, wave *S4*, speed 12 knots, $\beta = 180$ deg.

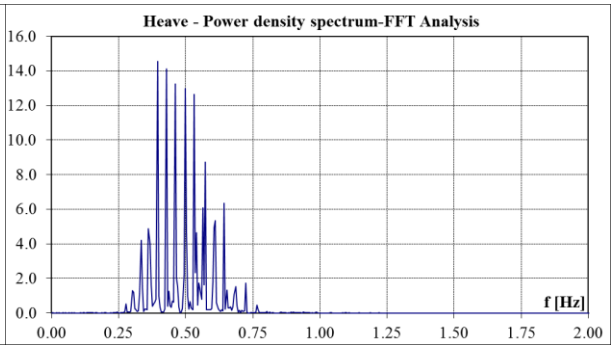

Figure 9b. Power density spectrum, heave motion, wave *S7*, speed 12 knots, $\beta = 180$ deg.

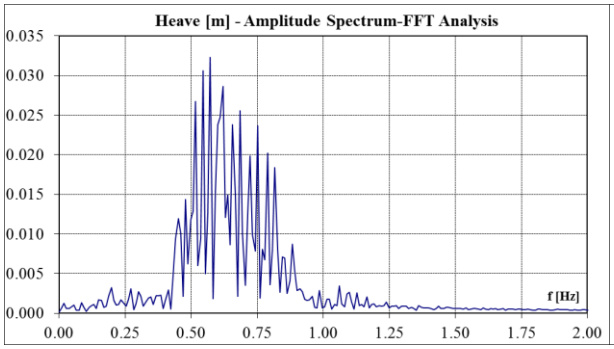

Figure 9c. Heave amplitude spectrum, wave *S4*, speed 12 knots, $\beta = 180$ deg.

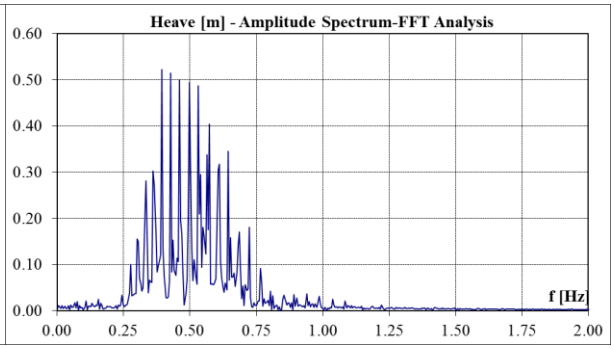

Figure 9d. Heave amplitude spectrum, wave *S7*, speed 12 knots, $\beta = 180$ deg.

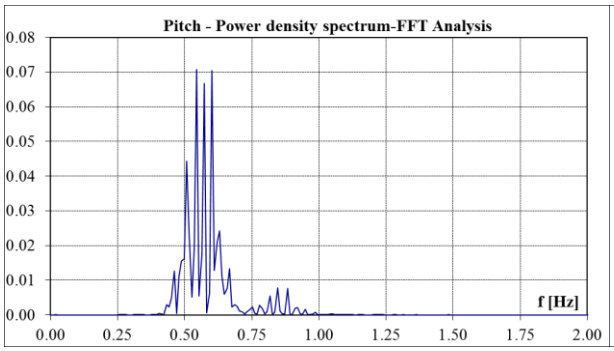

Figure 10a. Power density spectrum, pitch motion, wave *S4*, speed 12 knots, $\beta = 180$ deg.

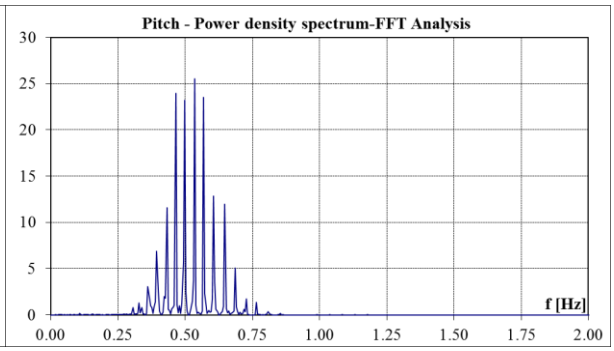

Figure 10b. Power density spectrum, pitch motion, wave *S7*, speed 12 knots, $\beta = 180$ deg.

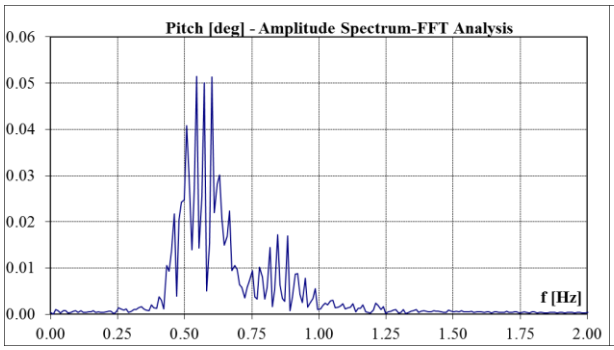

Figure 10c. Pitch amplitude spectrum, wave *S4*, speed 12 knots, $\beta = 180$ deg.

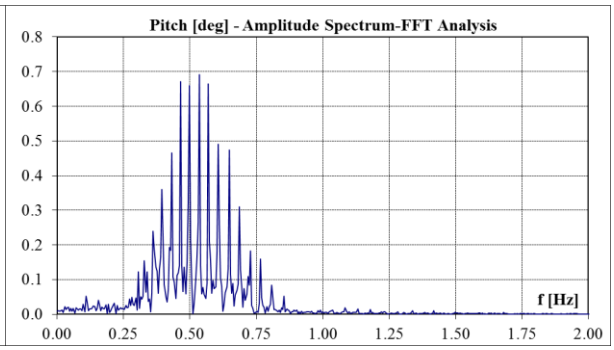

Figure 10d. Pitch amplitude spectrum, wave *S7*, speed 12 knots, $\beta = 180$ deg.

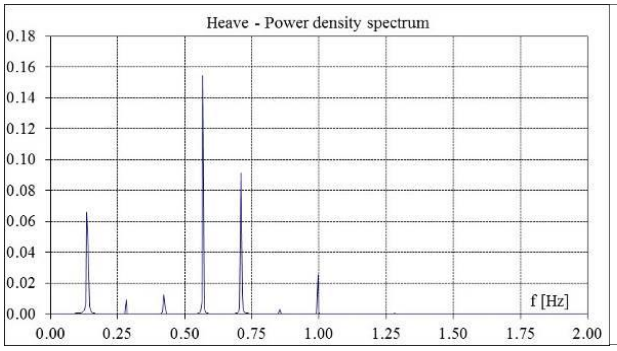

Figure 11a. Power density spectrum, heave motion, wave *S4*, speed 24 knots, $\beta = 180$ deg.

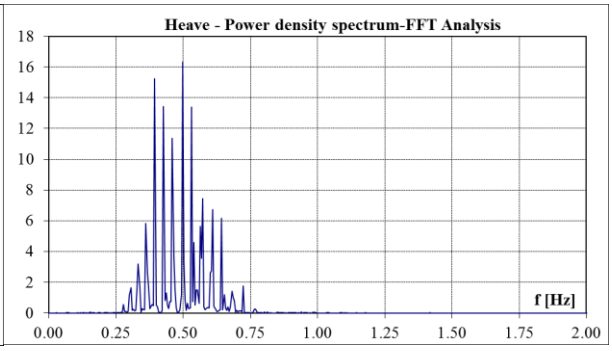

Figure 11b. Power density spectrum, heave motion, wave *S7,* speed 24 knots, $\beta = 180$ deg.

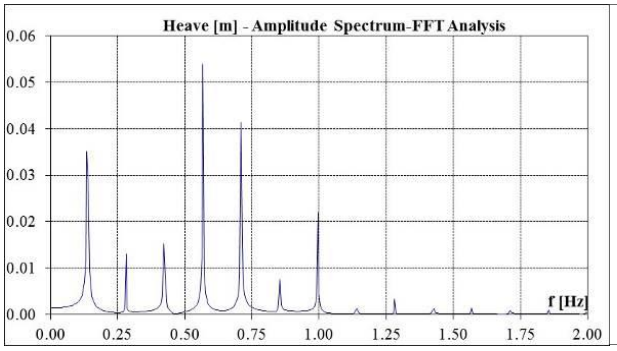

Figure 11c. Heave amplitude spectrum, wave *S4*, speed 24 knots, $\beta = 180$ deg.

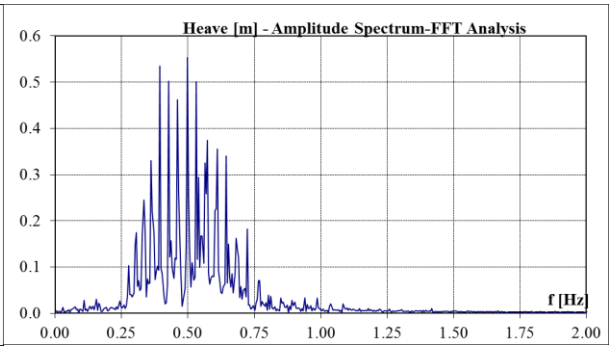

Figure 11d. Heave amplitude spectrum, wave *S7*, speed 24 knots, $\beta = 180$ deg.

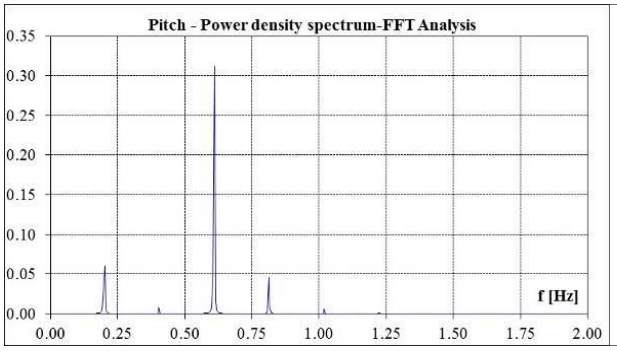

Figure 12a. Power density spectrum, pitch motion, wave *S4*, speed 24 knots, $\beta = 180$ deg.

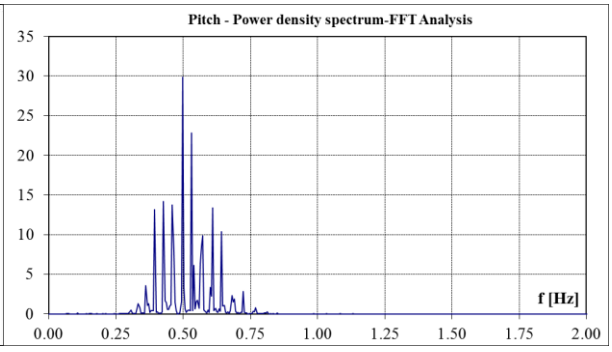

Figure 12b. Power density spectrum, pitch motion, wave *S7*, speed 24 knots, $\beta = 180$ deg.

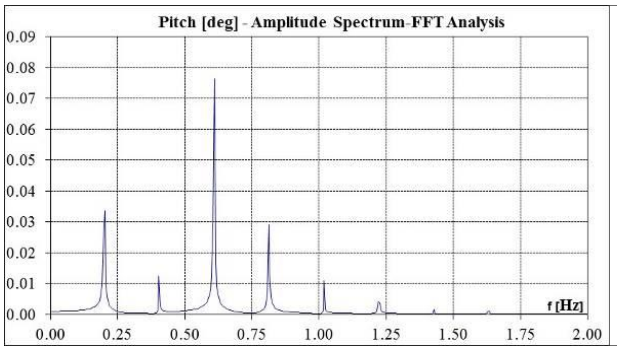

Figure 12c. Pitch amplitude spectrum, wave *S4*, speed 24 knots, $\beta = 180$ deg.

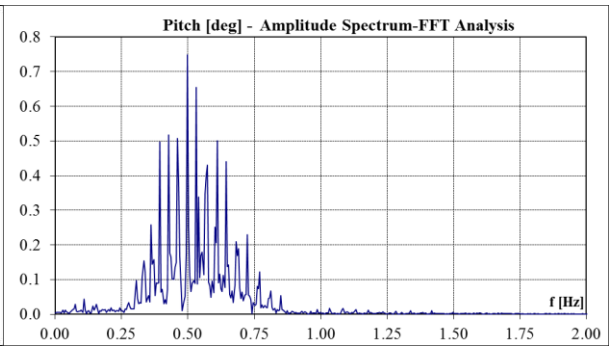

Figure 12d. Pitch amplitude spectrum, wave *S7,* speed 24 knots, $\beta = 180$ deg.

The seakeeping limit criteria are presented in equations (1)-(4).

$$RMS_{z\,max} = RMS_{heave} + (0.5 \cdot H_s)/2 \text{ at midship part, with admissible } RMS_{zadm}\text{=11.2m} \quad (1)$$

$$RMS_{z\,max} = RMS_{heave} + (L_{pp}/2 + x_F) \cdot RMS_{pitch} + (0.5 \cdot H_s)/2 \text{ at aft part, } RMS_{zadm}\text{=13.2m} \quad (2)$$

$$RMS_{z\,max} = RMS_{heave} + (L_{pp}/2 - x_F) \cdot RMS_{pitch} + (0.5 \cdot H_s)/2 \text{ at fore part, } RMS_{zadm}\text{=14.2m} \quad (3)$$

$RMS_{pitch\ adm}$=3 deg, the admissible pitch motion amplitude. (4)

For the sea states *S2..S7* (*Hs*=0.3…7.5m), heading angle 180 degrees, ship speed 12 knots, are given below, in Table 2, the operability criteria for the pitch and combined vertical displacement. Similar data are presented Table 3 for the maximum ship speed case of 24 knots.

Table 2. Operability criteria for the container ship, speed 12 knots.

Case/Sea state	**S2**	**S3**	**S4**	**S5**	**S6**	**S7**
H_s[m]	0.300	0.880	1.880	3.250	5.000	7.500
T_z[s]	5.300	6.200	0.620	6.900	8.800	10.700
RMS_{heave} [m]	0.024	0.127	0.264	0.610	1.614	3.970
RMS_z [m] midship	0.099	0.347	0.734	1.423	2.864	5.845
RMS_z [m] midhip / adm<=1	0.009	0.031	0.066	0.127	0.256	**0.522**
RMS_z [m] aft	0.062	0.422	0.893	2.222	3.225	12.155
RMS_z [m] aft / adm<=1	0.0047	0.0320	0.0676	0.1683	0.2443	**0.9209**
RMS_z [m] fore	0.071	0.487	1.032	2.580	3.583	13.974
RMS_z [m] fore / adm<=1	0.0050	0.0343	0.0727	0.1817	0.2524	**0.9841**
RMS_{pitch} [deg]	0.021	0.163	0.348	0.892	0.892	4.531
$RMS_{pitch} / RMS_{pitchadm} \le 1$	0.0071	0.0544	0.1159	0.2974	0.2974	**1.5105**

Table 3 Operability criteria for the container ship, speed 24 knots

Case/Sea state	**S2**	**S3**	**S4**	**S5**	**S6**	**S7**
H_s[m]	0.300	0.880	1.880	3.250	5.000	7.500
T_z[s]	5.300	6.200	0.620	6.900	8.800	10.700
RMS_{heave} [m]	0.152	0.163	0.212	0.514	2.070	3.954
RMS_z [m] midship	0.227	0.383	0.682	1.327	3.320	5.829
RMS_z [m] midhip / adm<=1	0.020	0.034	0.061	0.118	0.296	**0.520**
RMS_z [m] aft	0.359	0.633	1.132	2.572	7.904	14.069
RMS_z [m] aft / adm<=1	0.0272	0.0480	0.0857	0.1948	0.5988	**1.0658**
RMS_z [m] fore	0.388	0.689	1.232	2.848	8.923	15.900
RMS_z [m] fore / adm<=1	0.0273	0.0485	0.0867	0.2006	0.6284	**1.1197**
RMS_{pitch} [deg]	0.073	0.139	0.249	0.689	2.537	4.561
$RMS_{pitch} / RMS_{pitchadm} \le 1$	0.0243	0.0463	0.0829	0.2297	0.8458	**1.5205**

Base on the above data (tables 2,3), we can conclude that for the case of ship speed 12 knots, the values for RMS_z vertical combined motions are in limits, while the RMS_{pitch} pitch motion is above limits. Also, for the case of ship speed 24 knots, the RMS_z vertical combined motions and RMS_{pitch} pitch motion are above limits. This occurred at the sea state *S7* (*Hs*=7.5m) for both speed cases.

On overall waves range the motions (see figures 13a,b) are larger for the ship's speed of 24 knots in compare to the ship's speed of 12 knots.

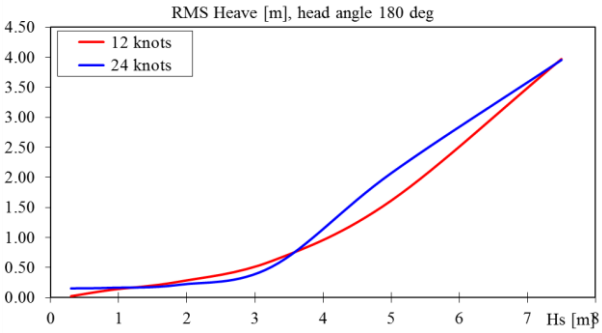

Figure 13a. *RMS* heave maximum values.

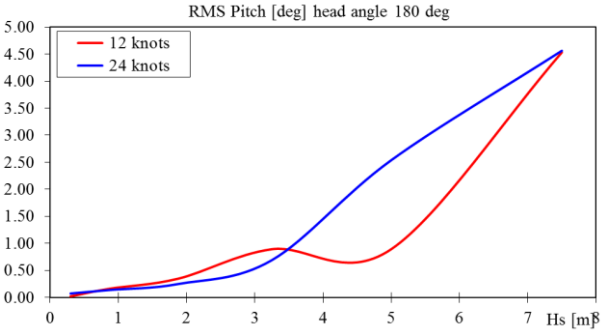

Figure 13b. *RMS* pitch maximum values.

5. Conclusions

The main conclusions drawn up from this study are the following:

1. Free-surface flow around the container ship was successfully computed. The ship's heave and pitch motions were computed by means of fully nonlinear potential flow solver, implemented by CFD – BEM approach.
2. The most significant ship hydrodynamic response on regular waves is in the case of lower frequency domain (see figures 4.a,b).
3. There is a good correlation between the experimental measurements and the numerical results, as can be seen in figures 5a,b.
4. The maximum values of *RAO*s occurred at the maximum speed case of 24 knots (figures 5a,b).
5. Using the CFD-BEM methodology for six sea states, described by *ITTC* wave spectrum (figure 7), the container ship dynamic response in irregular head waves was computed. The maximum dynamic response is obtained in the case of speed 24 knots (figures 11,12.a,b).
6. Imposing the operational seakeeping criteria from equations (1)-(4), the admissible navigation range is obtained. In the case of 12 knots speed, only the pitch criterion was exceeded, for sea state *S7* (*Hs*=7.5m), see table 2. In the case of maximum ship speed 24 knots, both seakeeping criteria were exceeded, for sea state *S7* (*Hs*=7.5m), see table 3.
7. Further studies shall include the oblique waves conditions and a wider range of ship's speed.

6. References

[1] Simonsen C D, Otzen J F, Nielsen C and Stern F 2014 CFD prediction of added resistance of the KCS in regular head and oblique waves, *30th Symposium on Naval Hydrodynamics, (Hobart, Tasmania, 2-7 Nov.2014)*
[2] International Towing Conference (ITTC), https://ittc.info
[3] Ogilvie T F and Tuck EO 1969 *A Rational Strip Theory of Ship Motion: Part I, Report 013* Department of Naval Architecture, Michigan USA
[4] Salvesen N, Tuck E O and Faltinsen O 1970 Ship Motion and Sea Loads, *The Annual Meeting of Society Naval Architects and Marine Engineers (Detroit, Mich., July 20-22, 1970)*
[5] Hess J L and Smith A M O 1966 Calculation of Potential Flow about Arbitrary Bodies, *Progress in Aeronautical Sciences* **8** 1-138
[6] Janson C-E 1997 *Potential Flow Panel Methods for the Calculation of Free-surface Flows with Lift* PhD Thesis, Chalmers University of Technology Gothenburg

[7] Jensen G 1987 On the Numerical Radiation Condition in the Steady-State Ship Wave Problem, *Journal of Ship Research* **31(1)** 14-42
[8] https://www.flowtech.se/, User Manual - Shipflow Motions 6.4, 2017
[9] Domnisoru L 2001 *Ship dynamics. Oscillations and vibrations* (Bucharest: Technical Pub. House)
[10] Lungu, A and Raad P 1998 Non-linear Potential Free-Surface Flow Around the Series-60 Ship Hull, *1998 ASME Fluids Engineering Division Summer Meeting FEDSM'98 (June 21-25, 1998 Washington DC*)